6ICEGE 6th International Conference on Earthquake Geotechnical Engineering
1-4 November 2015
Christchurch, New Zealand

Contribution of Geostatistical Technique to Investigate the Spatial Variation of Liquefaction Potential in Urayasu City, Japan

R. M. Pokhrel[1], T. Kiyota[2] and K. Kajihara[3]

ABSTRACT

Following the 2011 Off the Pacific Coast of Tohoku Earthquake (M_W=9), Urayasu City in Chiba Prefecture, Japan, which is geologically composed of young reclaimed land, experienced severe soil liquefaction. The major problems associated with liquefactions were ground subsidence, tilting of houses, buckling of roads and lifelines cut off. To gain a better understanding into these phenomena, a detailed study on liquefaction assessment for future earthquakes is important for such damaged area. To this scope, in this paper, the contribution of GIS technique to analyze the spatial distribution of liquefaction potential is presented. Available 109 boreholes were used to study the liquefaction potential of the Urayasu City. Using geostatistical techniques in GIS, the spatial distribution of liquefaction potential map were prepared indicating zones with different liquefaction potential classes. In the analysis, the anisotropy of the data set clearly reflects the difference between old deposit area and reclaimed area, as well as the reclamation history, of Urayasu City.

Introduction

Soil liquefaction is an earthquake-induced ground failure mechanism that mostly occurs in loose, saturated granular sediments (particularly sand and silty sand). It may induce severe ground subsidence, lateral spreading, tilting of super structures and uplift of light underground structures especially in young alluvial (Holocene) deposits and reclaimed land. For example, Urayasu City in Chiba Prefecture, Japan, which is geologically composed of recently reclaimed land (the reclamation in this area was completed between 1966 and 1985), suffered from severe liquefaction at the time of 2011 Off the Pacific Coast of Tohoku Earthquake (M_W = 9.0). To be precise, about 85% of the Urayasu city was heavily damaged due to liquefaction (Yasuda et al., 2012).

In Urayasu City, soil dredged from the sea bed was filled to the height of about sea level in the reclamation work. Then, it was covered with sandy soils transported by boat from Boso Peninsula (Yasuda et al., 2012). For that reason, the soil in the Urayasu reclaimed land area was highly prone to liquefaction during the 2011 earthquake. Fig. 1 shows a manhole uplifted due to liquefaction occurrence in 2011 in Urayasu City. Sand boiling was frequently observed in the city, causing significant ground subsidence. Based on the reclamation history, Urayasu City can be divided into three areas, namely Motomachi area, Nakamachi area and Shinmachi area, as

[1]JSPS Postdoctoral Research Fellow, Institute of Industrial Science, University of Tokyo, Japan, pokhrel@iis.u-tokyo.ac.jp
[2]Associate Professor, Institute of Industrial Science, University of Tokyo, Japan, kiyota@iis.u-tokyo.ac.jp
[3] Graduate student, Yokohama National University, Japan, k-kaji@iis.u-tokyo.ac.jp

shown in Fig. 2. In this paper, a detailed study is presented for evaluating the spatial distribution of liquefaction potential in Urayasu City. To do so, available 109 field boreholes data (shown in Fig. 2 as red dots) were collected and the liquefaction potential was calculated for each borehole location. Then, a geostatistical method of interpolation in a Geographic Information System (GIS) was used to evaluate the spatial distribution of liquefaction potential. In addition, anisotropic characteristics of the data set were investigated, which would link with soil characteristics as well as reclamation history of Urayasu City.

Figure 1: Manhole uplifted during the 2011 Off the Pacific Coast of Tohoku earthquake in Urayasu City.

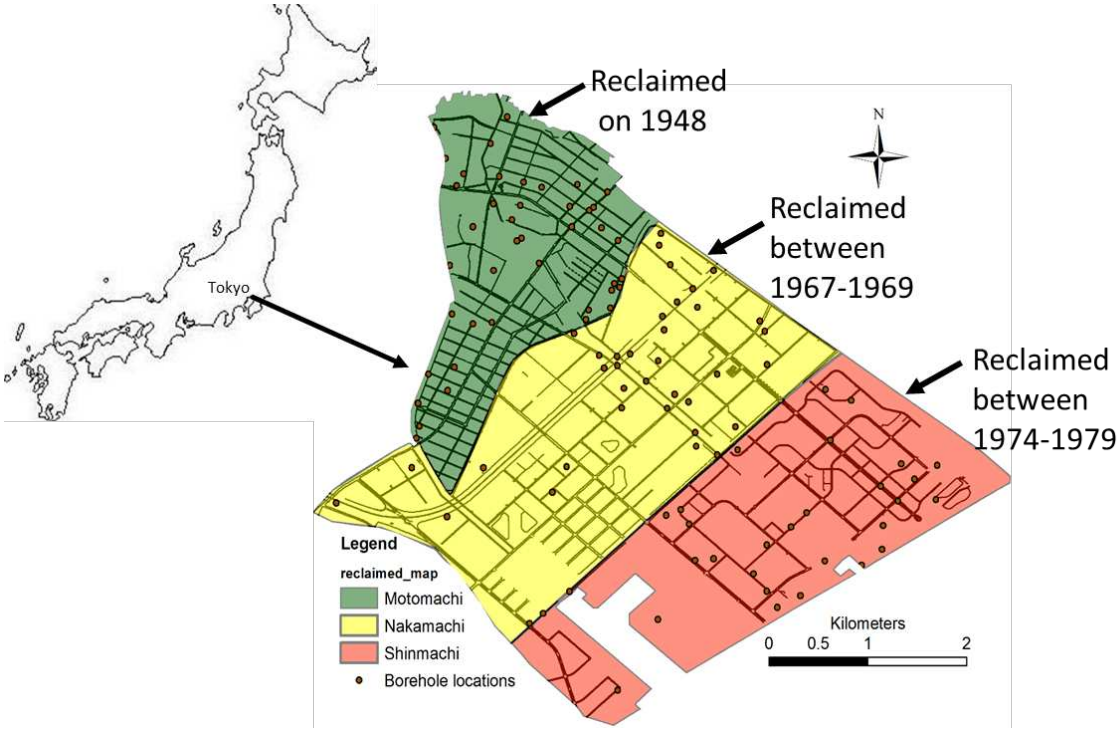

Figure 2: Reclamation history of Urayasu City and location of boreholes used in this study (Urayasu city, 2012; Chiba Prefecture, 2014).

Methodology and Analysis

Liquefaction potential at boreholes

For the liquefaction potential zoning, the main step is the collection and calculation of geotechnical data from boreholes. In this paper, the liquefaction resistant parameter was evaluated by using Road Bridge manual, Japan (2002, 2012) which is widely used for the liquefaction assessment in Japan. This method compares the cyclic resistance ratio of insitu sands with cyclic stress ratio induced by seismic activity. The liquefaction resistance factor for a given soil layer is evaluated using standard penetration test (SPT) results. Moreover, the liquefaction potential at each sampled borehole location is quantified by an index called the liquefaction potential index (P_L) proposed by Iwasaki et al. (1982) where the P_L value is varied from 0 to 100. Finally, a data table containing the coordinates and P_L values at each borehole was prepared for GIS analysis.

Geostatistics for interpolation

A liquefaction potential surface is a continuous field of values that may vary over an infinite number of points. Thus, it is very difficult to measure and record the liquefaction potential value at every point. Therefore, in this study, the geostatistical method was used to interpolate the liquefaction potential at unsampled locations. This study used a kriging method for the interpolation, which is an exact and powerful interpolation method in geostatistics. For the kriging method, the first step is to examine the data in order to identify the spatial structure, which is often represented by the empirical semivariogram (Isaaks and Srivastava, 1989). A semivariogram is a plot that shows the relationship between semivariance and distance between all the pairs of available data points, as schematically illustrated in Fig. 3. The experimental semivariance for liquefaction potential was calculated using Eqn. 1 (Pokhrel et al. 2012, 2013):

$$\gamma(h) = \frac{1}{2N(h)} \sum_{i=1}^{N(h)} \left(P_L(i) - P_L(i,h)\right)^2 \quad (1)$$

where $\gamma(h)$ is the estimated value of the semivariance for distance of h; $N(h)$ is the number of experimental pairs separated by h; $P_L(i)$ and $P_L(i,h)$ are the values of the variables P_L at (i) and (i,h) positions, respectively.

Once the model variogram is constructed, it can be used to compute the weight for P_L values. This weight is used to evaluate the liquefaction potential at any point in the study area by using Eqn. (2):

$$p_L(x,y) = \sum_{i=1}^{n} \lambda_i(x_i, y_i)\, p_L(i) \quad (2)$$

where $P_L(x,y)$ is the P_L at (x,y) estimated by the interpolation; $P_L(i)$ is the evaluated P_L value at the i^{th} location; $\lambda_i(x_i,y_i)$ is the weight for $P_L(i)$ to estimate $P_L(x,y)$; n is the number of locations used for the kriging interpolation. In the kriging method, weights are based not only on the

distance between the measured points and the prediction location but also on the overall spatial relationships among the measured values around the prediction location, as shown in the variogram model in Fig. 3.

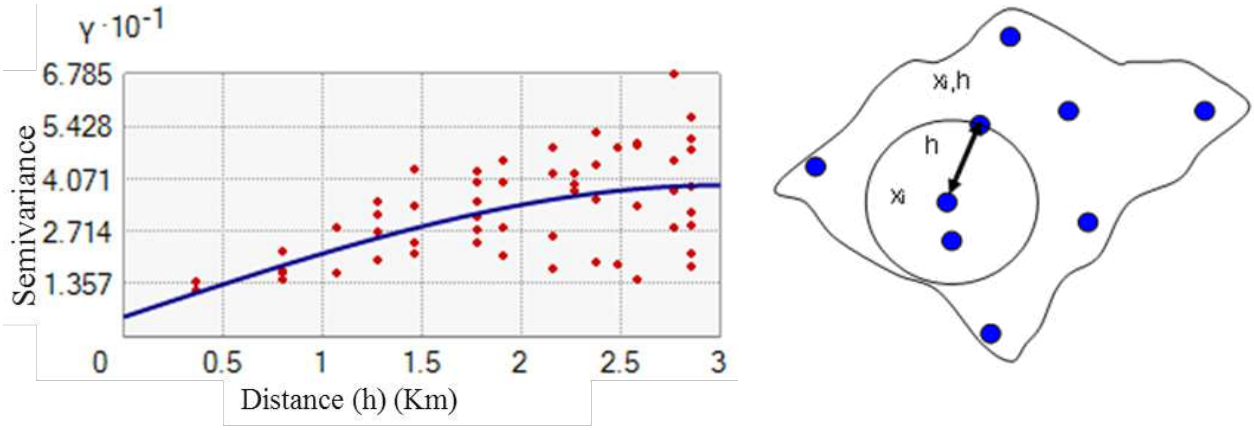

Figure 3: Kriging variogram model.

The kriging method weights the surrounding measured values to derive a prediction for an unsampled location. To estimate the weight values for the surrounding measured locations, the experimental data point semivariogram shown in Fig. 3 was constructed from the measured values. These data points provide the relationship between points on the surface. Then, using the variogram model, the curve line in Fig. 3 was derived by fitting the experimental variogram.

Note that, in Fig. 3, it was assumed that the ground is isotropic, which means that the changes of P_L values in all directions are the same; and therefore, the spatial correlation structure is the same in all directions. In this case, the semivariogram model depends on the magnitude of the distance, but not on the direction. The directional effects on the data set are known as anisotropy (Fig. 4).

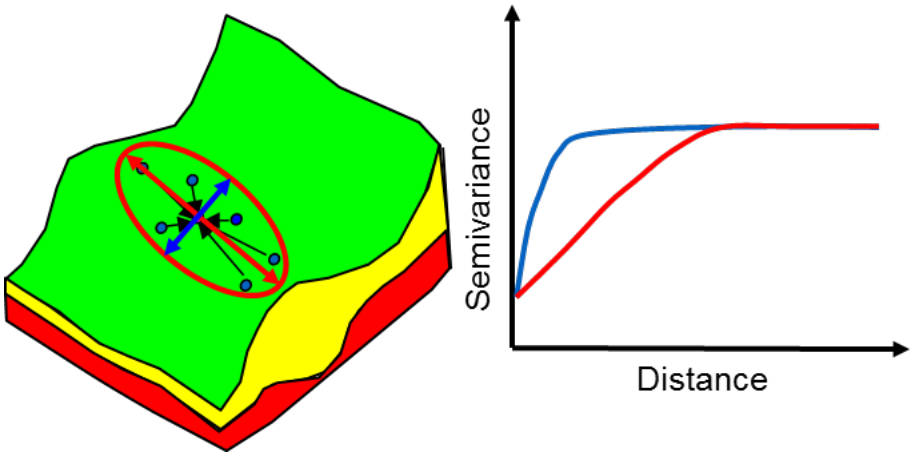

Figure 4: Schetamatic diagram for anisotropic model.

Anisotropy

To check for the directional anisotropy in an experimental semivariogram, the semivariance values are calculated for pairs of data falling within certain directional bands, as shown in Fig. 5, which will be most reflected by the ground conditions. In Fig. 5a), the points along the direction of N60^{0}East were examined. The data set along this direction shows similar properties (low semivariance value) for the long distance. This influence will affect the points of the semivariogram and the model that will be fitted as shown in Fig. 6a). The weight value λ for this direction was estimated by using the regression curve. Similarly in Fig. 5b) the data sets along the direction of N30^{0}West were examined and plotted in Fig. 6b). It shows the semivariance value increases with distance more rapidly than that in Fig. 6a) in the direction of North 30^{0}West before it becomes constant. In this direction, the liquefaction potential value changes lager than that in the direction of N60^{0}East in the same distance. The semivariogram data in Fig. 6, indicates that the empirical variogram will express the geospatial anisotropy in the investigated areas.

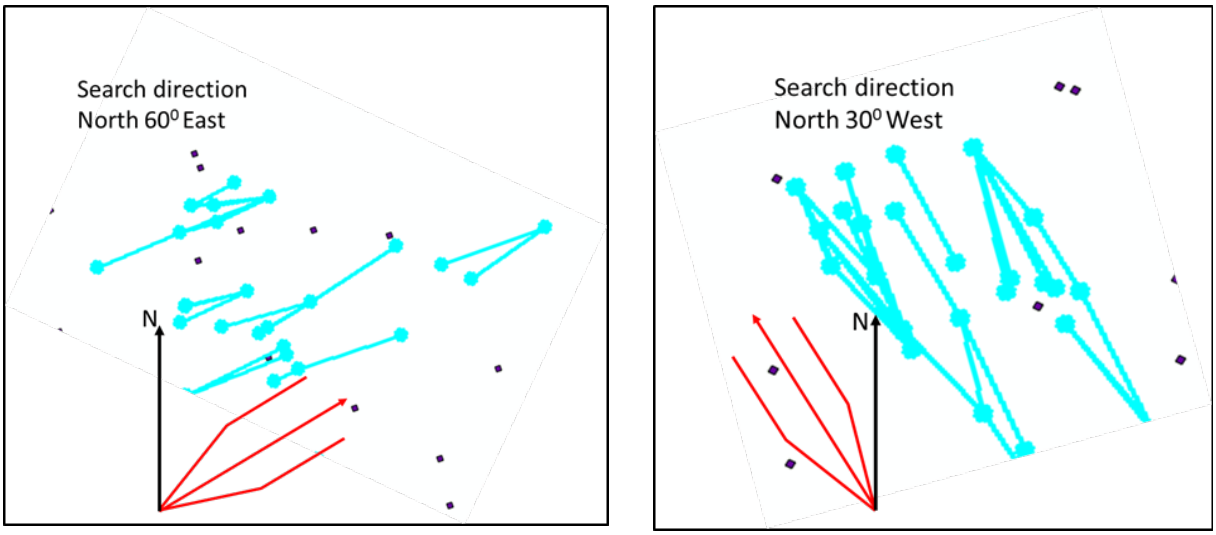

a b

Figure 5: Anisotropic direction a) N 60^0 East and b) N 30^0 West.

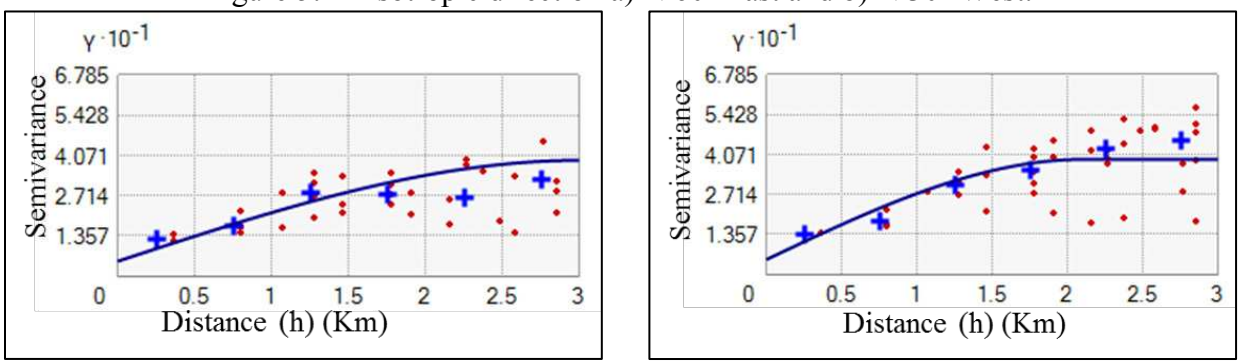

a b

Figure 6: Semivariogram curves for different direction (a) along direction N60^0 East (b) along direction N30^0 West.

In the case of the model curve fitted for this empirical semivariogram, data also change their shape according to the direction. Thus, the weight value estimated from these curves in Fig. 6 were also adjusted to the direction. In the kriging method, to avoid a biased estimation, the summation of the weight for all the surrounding points should be equal to 1. In Fig. 6, it is clearly observed that the longest range is in the direction of $N60^0$East and the shortest range is in the $N30^0$West. Therefore, the highest weight value for the observation point along $N60^0$East and lowest weight value for the point in the direction of $N30^0$West should be considered. After considering the anisotropic direction of the ground, a spatial distribution map of liquefaction potential of the Urayasu City was prepared.

Results

The spatial variation of liquefaction potential map, prepared as described in the previous section, is shown in Fig. 7. In the analysis, the peak ground acceleration 174.3 gal (resultant values of X, Y and Z components) at K-net Urayasu station (N35.6537deg., E139.9023deg.) was used for Motomachi area. For Nakamachi and Shinmachi areas, 200gal was assumed as a peak ground acceleration based on the one-dimentional seismic response analysis RSPM, reported by Ishikawa et al. (2014). A total of 109 boreholes were used for Urayasu City without knowing the reclamation history.

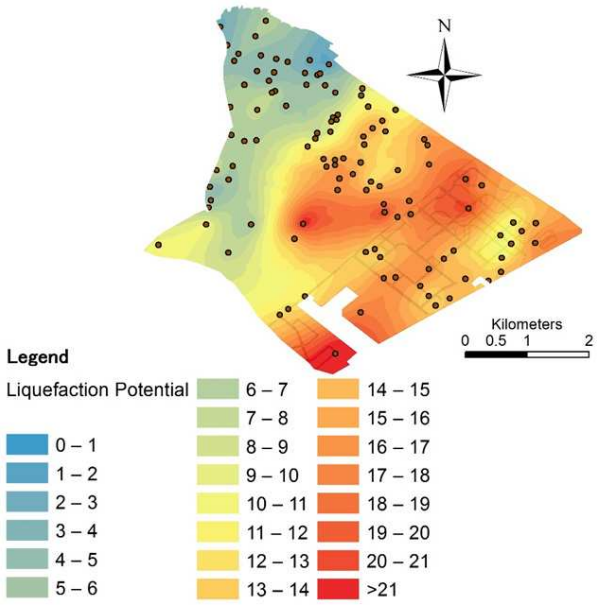

Figure 7: Liquefaction potential distribution map of the Urayasu City.

From Fig. 7, it can be seen that most of the area is zoned as high liquefaction potential area. The area with natural or alluvial deposit has low or no liquefaction. During the 2011 earthquake, most of Urayasu City experienced severe liquefaction except for the natural soil deposits. The resultant map shown in Fig. 7 seems to be consistent with the reclamation history in Fig. 2. The reclamation history map shows that there are mainly three different reclamation works. Motomachi area has thick natural soil deposit covered with thin reclaimed (reclaimed on 1948)

soil, therefore, this area falls into low liquefaction potential zone. Since Nakamachi (reclaimed on 1967-1969) and Shinmachi (Reclaimed on 1974-1979) areas have thick reclaimed soil deposits, these areas have high liquefaction potential. The different reclaimed works are clearly reflected from the analysis. This anisotropic direction of the ground implies that the soils in the same reclamation area have similar characteristics.

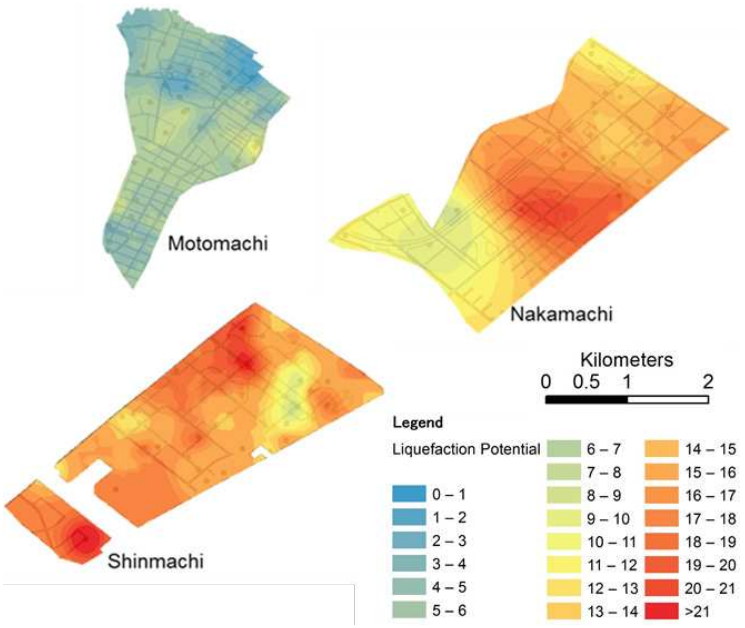

Figure 8: Liquefaction potential of the individual area.

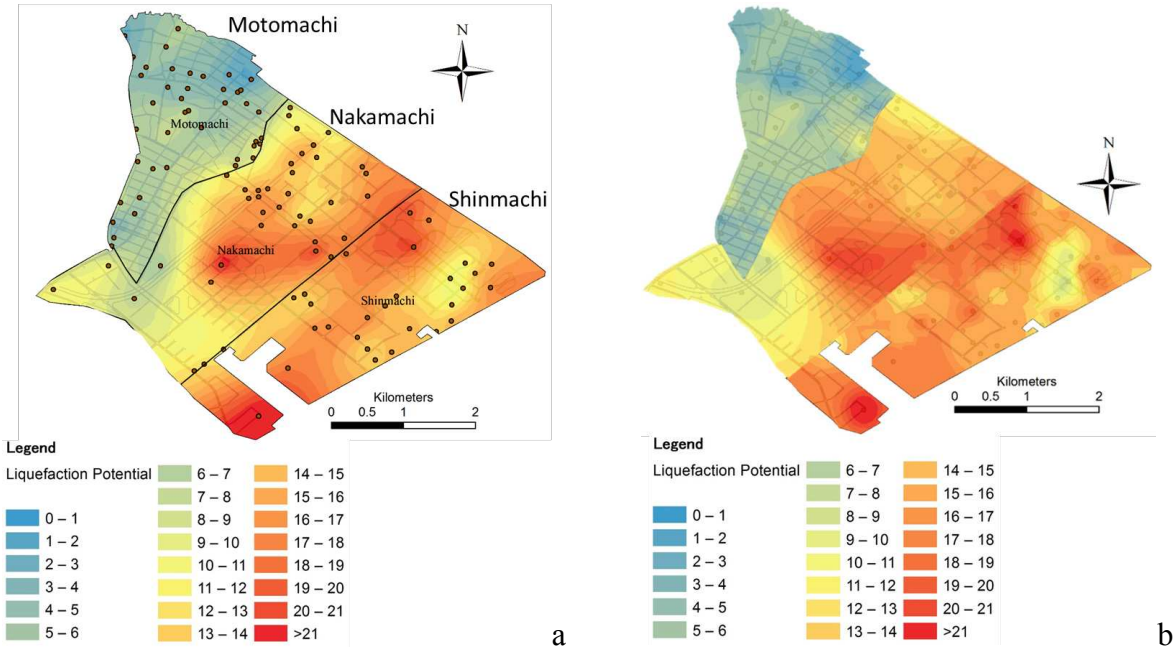

Figure 9: Liquefaction potential map of Urayasu City a) a map without knowing reclamation history (c.f. Fig. 7), b) a map pieced together the individual map (c.f. Fig. 8).

Furthermore, to check the validity of the proposed analytical methods, this study conducted the same analyses for the individual areas, Motomachi area, Nakamachi area, and Shinmachi area, separately. The sampled boreholes within the corresponding individual areas were used to interpolate the liquefaction potential and prepare the liquefaction potential map individually, as shown in Fig. 8. As a result, Motomachi area shows low liquefaction potential, while Nakamachi and Shinmachi areas fall into high liquefaction potential zone.

Following, the maps in Fig. 8, were then compared to the resultant liquefaction potential map. Fig. 9 shows the comparison of the two maps. Figure 9a) shows the map prepared by considering the entire Urayasu City as a single area (without knowing the reclamation zones) and Fig. 9b) shows the map combining the individual maps in Fig. 8, considering the different reclamation history. These two maps match well, indicating that the method used to interpolate liquefaction potential considering anisotropic direction in Urayasu City is rational.

Conclusions

A liquefaction potential map offers valuable information concerning earthquake hazards and their mitigation. This study proposed a geostatistical interpolation method in GIS, which takes into account geospatial anisotropy for the liquefaction potential map. The prepared spatial distribution of P_L value in Urayasu City is consistent with the reclamation history of the city. The result shows that the young reclamation areas (Nakamachi and Shinmachi) have high liquefaction potential, while the old reclamation and alluvial deposits (Motomachi) area is zoned as low liquefaction potential area. This result is consistent with the observed liquefaction aspects in Urayasu City during the 2011 Off Pacific Coast of Tohoku Earthquake.

Acknowledgments

The authors are grateful to the Japan Society for the Promotion of Science (JSPS) for the JSPS Postdoctoral Fellowship supporting this research. Some of the borehole data and relevant experimental data were provided by the Technical Committee on measures against liquefaction (chaired by Prof. Ishihara) organised by Urayasu city. The authors would also like to thank Dr. Chiaro Gabriale for his valuable suggestions on the manuscript.

References

Chiba Prefecture, *Geotechnical Environment Information Bank in Chiba Prefecture,* URL http:// www.pref.chiba.lg.jp/suiho/chishitsu.html, accessed in 2014. (in Japanese)

Isaaks, E.H., Srivastava, R.M., An Introduction to Applied Geostatistics, *Oxford University press*, Oxford, 561 pp, 1989.

Ishikawa, K., Yasuda S., Ikarashi, s., Study on the reasonable liquefaction prediction of Urayasu in case of the Great East Japan Earthquake based on Representative Soil Profile Models, *The 14th Japan Earthqauke Engineering Symposium,* 2014. (in Japanese)

Iwasaki, T., Tokida, K., Tatsuoka, F., Watanabe, S., Yasuda, S., and Sato, H., Microzonation for soil liquefaction potential using simplified methods, *Proceedings of 3rd International Earthquake Microzonation Conference,* Seattle, pp. 1319-1330, 1982.

Japan Road Association, Specifications for Highway Bridges, seismic design, 2002, Part V.

Japan road association, *Seismic designed specifications for Highway Bridge* 2012, volume V. (in Japanese)

Pokhrel, R.M., Kuwano, J., Tachibana, S. Geostatistical analysis for spatial evaluation of liquefaction potential in Saitama City, *Lowland Technology International, ,* vol. **14**, No.1, pp. 45-51, 2012.

Pokhrel, R.M., Kuwano, J., Tachibana, S. A kriging method of interpolation used to map liquefaction potential over alluvial ground, *Engineering Geology,* Vol. **152**, pp. 26-37, 2013.

Urayasu City, *Data compiled by the Technical Committee on measures against Liquefaction,* URL http://www.city.urayasu.chiba.jp/menu11324.html, 2012 (in Japanese).

Yasuda, S., Harada, K., Ishikawa, K, Kanemaru, Y., Characteristics of liquefaction in Tokyo Bay area by the 2011 Great East Japan Earthquake, *Soils and Foundations,* Vol. **52**(5), pp. 793-810, 2012.